Influence of corrosion crack patterns on the rate of crack widening of RC beams

Goitseone Malumbela [a,*], Pilate Moyo [b], Mark Alexander [b]

[a] Dept. of Civil Eng., Univ. of Botswana, Pjbag 0061, Gaborone, Botswana
[b] Dept. of Civil Eng., Univ. of Cape Town, Pjbag X3, Rondebosch 7700, South Africa

A B S T R A C T

Corrosion crack widths are often used by structural engineers in the field to predict level of steel corrosion as well as residual load-bearing capacities of corroding RC structures. This paper presents further work on this matter but with focus on corrosion crack patterns and how they affect rate of crack widening. It is based on results from a research where 17 quasi-full-scale (153 × 254 × 3000 mm) RC beams were corroded under various levels of sustained loads. The rate of widening of corrosion crack widths was found to be very much dependent on crack patterns. Deformation of cover concrete under each crack pattern was discussed. It was found that at maximum crack widths below 0.6 mm, the majority of beams exhibited nearly similar crack patterns as well as rate of widening of corrosion cracks. A mass loss of steel of 1% corresponded to a maximum crack width between 0.14 and 0.22 mm. At large crack widths (>0.6 mm), various beams exhibited very different rates of crack widening. It was shown that at crack widths above 0.6 mm, to be conservative an increase in mass loss of steel of 1% corresponded to corrosion crack widening of 0.02 mm.

Keywords:
Reinforced concrete
Crack patterns
Crack widths
Steel corrosion

1. Introduction

Corrosion of reinforcing steel embedded in concrete probably provides structural engineers and asset managers with the most threatening problem because it deteriorates load-bearing capacity of RC structures. They however, appreciate that in reducing their load-bearing capacity, it gives out measurable indicators of its occurrence. Researchers worldwide continue to try and identify these indicators and to develop their relations with level of steel corrosion as well as with load-bearing capacities of corroding RC structures. Stiffness is one of the indicators of corrosion that has received wide research. Its major shortcoming is that it is very much influenced by the testing procedure used. For example, when monitored on in-service structures whilst they corrode under load, it is limited to indicating levels of steel corrosion at low levels of corrosion (<7% by mass loss of steel) [1–4]. However, if at a chosen level of steel corrosion stiffness is tested by subjecting corroded specimens to a monotonically increased static load, Zhang et al. [5] have shown that it can indicate up to mass losses of steel of 40%. Unfortunately structural engineers are more interested in changes in stiffness due to an increase in the level of steel corrosion. Contrary to stiffness, corrosion crack widths have been shown to always effectively increase with level of steel corrosion. Understandably, more research has been devoted to studying them. The following section summarises previous research on relation between corrosion crack widths and level of steel corrosion.

2. Previous work on corrosion crack widths

One detailed work to relate widths of corrosion cracks with level of steel corrosion was presented by Torres-Acosta and Martinez-Madrid [6]. In their publication, they compiled data in the literature on the interaction between maximum crack widths and level of steel corrosion. Since the various researchers from whom they obtained the data used different experimental procedures, it is not surprising that the relation they obtained had a large scatter. However, they found a defined trend that indicated corrosion crack widths to linearly increase with an increase in level of steel corrosion. From this trend, it can be shown that a mass loss of steel of 1% corresponded to a maximum crack width of 0.03 mm. Other researchers (not included in Torres-Acosta and Martinez-Madrid [6]) such as Alonso et al. [7], also found widths of corrosion cracks to linearly increase with level of steel corrosion. They however, contended that a mass loss of steel of 1% corresponds to a maximum crack width between 0.04 and 0.08 mm. El Maaddawy and Soudki [8] found mass loss of steel of 1% to yield maximum corrosion cracks from 0.08 to 0.14 mm. In agreement with above results, Badawi and Soudki [9] found mass loss of steel of 1% to correspond to crack widths from 0.1 to 0.14 mm.

It should be mentioned that above relations have been used by some researchers to predict residual load-bearing capacities of corroding RC structures [10]. Their major drawback however, is

* Corresponding author. Tel.: +267 355 4332; fax: +267 395 2309.
E-mail address: malumbela@mopipi.ub.bw (G. Malumbela).

that whilst corrosion crack widths were measured at a particular location of a corroding RC member so as to identify maximum crack width, mass loss of steel was taken as an average loss within the corroded region. From a structural mechanics viewpoint, load-bearing capacity of a corrosion-affected RC structure is related to maximum loss in cross-sectional area of steel. The interest of researchers should therefore be to relate maximum crack width with maximum loss of steel.

In order to further understand cracking behaviour of corroding RC structures, some researchers studied pattern of corrosion cracks. Alonso et al. [7] found that when a corroding steel bar was placed at the corner of a concrete specimen so that it had equal covers on the two near-faces, the first corrosion cracks simultaneously-appeared in both faces and propagated parallel to steel bars. When cover depths were varied, they found cracks to appear on the face nearest the corroding bar. In a similar work, El Maaddawy and Soudki [8] studied patterns of corrosion cracks in corroding RC specimens but with two corroding bars. The bars had centre-to-centre spacing of 80 mm and concrete covers of 25 mm on the side and top face of beams. For all samples, they initially observed two corrosion cracks near each corroding bar, and each crack propagated parallel to the bar. These cracks were either on the top face or on the side face. Interestingly, when the level of steel corrosion was increased, a third crack appeared next to a corroding bar but on a face that was uncracked. This indicates that the pattern of corrosion cracks changes with an increase in the level of steel corrosion.

Cabrera [11] also monitored crack patterns but on corroded RC slabs with different cover depths. Their specimens were reinforced with three steel bars with centre-to-centre spacing from 98 to 124 mm. Cover depths of steel bars were also varied. They found crack widths on all slabs to develop parallel to each corroding bar. When cover depths on side faces and on the tensile face were varied, cracks were only observed on the face nearest the corroding bar. However, when covers were equal, exterior bars either exhibited a crack on the side face or on the tensile face but not on both faces. Similar crack patterns but on beams that were corroded under load were observed by other researchers such as Ballim et al. [1,2], El Maaddawy et al. [12] and Zhang et al. [5,13,14].

Without understanding implications of these crack patterns on rate of widening of corrosion cracks, rate of steel corrosion, and behaviour of corroded structures, there is little value in studying them. Unfortunately, in studying corrosion crack patterns, many researchers only prepared crack maps and measured crack widths at the end of corrosion tests [1,2,6,11]. For the few who continuously measured widening of corrosion cracks, they limited their measurements to a few points on the cover concrete [9,12]. This

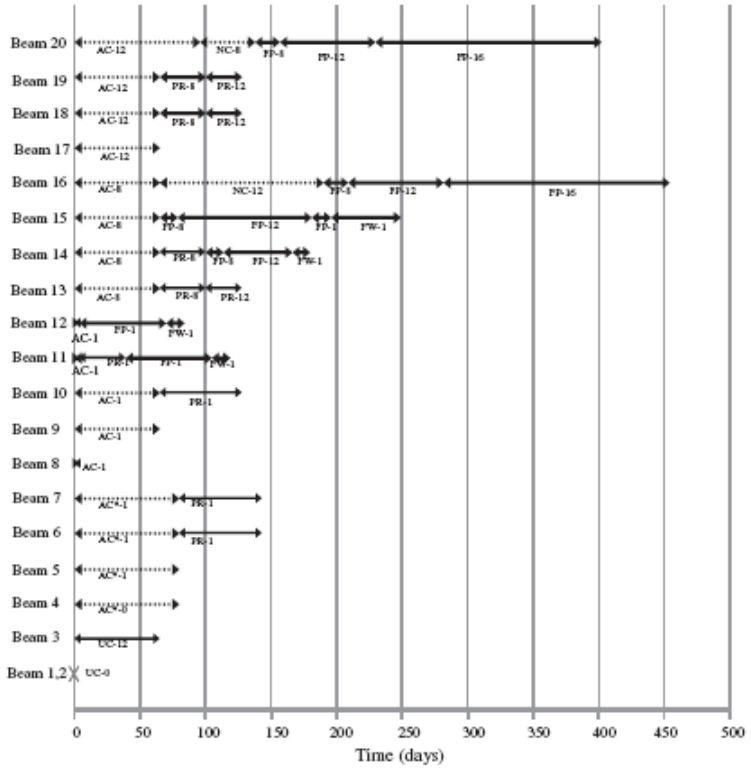

Designation: UC = uncorroded; AC* = accelerated corrosion with 4-day drying cycles; AC = accelerated corrosion with 2-day drying cycles; NC = natural steel corrosion; PR = patch repair; FP = repair with FRP plate; FW = wrap beam and FRP plate with FRP sheets; and a number after the two letters indicates the level of sustained load as a percentage of the load-bearing capacity of a control beam.

Fig. 1. Schematic of the experimental programme.

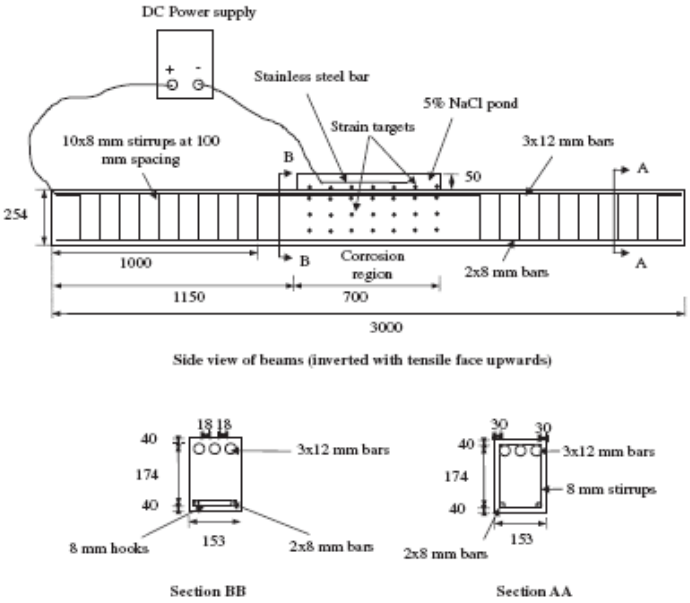

Fig. 2. Reinforcement configuration.

paper presents and discusses results from an extensive research that was conducted to evaluate influence of corrosion crack patterns on rate of widening of cracks. It also discusses mechanisms of deformation of cover concrete due to corrosion of embedded steel.

3. Experimental programme

Detailed discussion on the experimental programme of the research is in Malumbela et al. [4,15,16]. To help the reader, only a summary of the programme is given here. The overall experimental programme involved testing 20 quasi-full-scale RC beams ($153 \times 254 \times 3000$ mm). A schematic of the programme is shown in Fig. 1. As shown in the figure, beams were tested under five different levels of sustained loads: 0%, 1% (low deflections), 8% (high deflections but no flexural cracks) and 12% and 16% (high deflections and flexural cracks) of the ultimate load-bearing capacity of a non-corroded beam. Discussions on this paper are on beams 4–20 but limited to their results during accelerated corrosion. These results will, in subsequent publications, be compared to those under natural steel corrosion. As indicated in Fig. 1, some beams are still under test. Details of loading rigs used in this research are discussed in Malumbela et al. [4,15].

Reinforcement configuration is shown in Fig. 2 and the compressive strength of concrete used is in Table 1. Longitudinal tensile steel bars used were of 12-mm diameter and had yield strength of 549 MPa (standard deviation (s.d.) = 3 MPa) and ultimate strength of 698 MPa (s.d. = 4 MPa). Compression steel bars were of 8-mm diameter and had yield strength of 385 MPa (s.d. = 1 MPa) and ultimate strength of 451 MPa (s.d. = 2 MPa).

Two sequential corrosion processes were used; firstly accelerated corrosion (designated AC is Fig. 1) by impressing an anodic current (current density of 189 $\mu A/cm^2$) followed, in selected beams, by natural steel corrosion (designated NC is Fig. 1). Accelerated corrosion was divided into two processes; one with four-day wetting cycles with salt solution followed by two-day drying cycles and another where four-day drying cycles were used instead. For the majority of beams, anodic current was impressed for 44 days to achieve a theoretical loss of steel of about 10%. The total accelerated corrosion days, including drying days, were 64 days for beams with two-day drying cycles and 84 days for those with four-day drying cycles. In beams 8, 11, and 12 corrosion was limited to the time of first appearance of a visible corrosion crack. This was

Table 1
Experimental results on crack patterns.

Beam No.	f'_c, MPa (s.d.)	Sustained load as % of ultimate capacity during accelerated corrosion phase	Crack pattern
4[a]	46.5 (1.1)	0%	B
5[a]	35.0 (1.2)	1%	
6[a]	46.6 (1.1)		
7[a]	46.6 (1.1)		
8	40.2 (1.2)		A
9	38.9 (1.4)		C
10	38.9 (1.4)		
11	35.2 (0.8)		A
12	46.6(1.4)		
13	35.2 (0.8)	8%	B
14	40.1 (1.3)		
15	40.1(1.3)		
16	40.1 (1.3)		A
17	40.1 (1.3)	12%	C
18	40.0 (1.1)		B
19	40.0 (1.1)		
20	40.2 (1.2)		

f'_c = compressive strength of concrete.
S.d. = standard deviation.
[a] Four-day drying cycles.

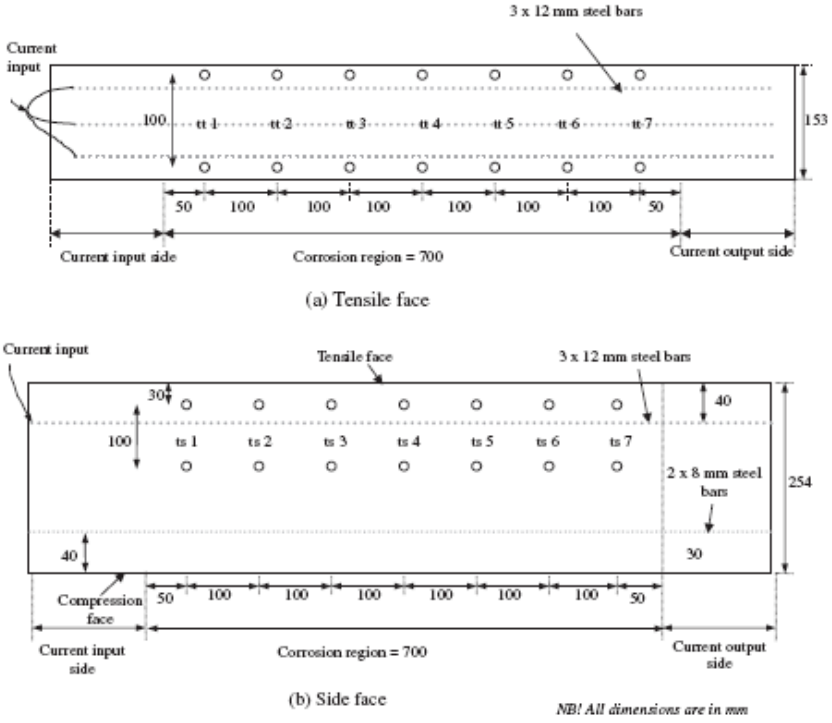

Designation: tt = transverse strains on the tensile face; and ts = vertical strains on the side face

Fig. 3. Location of targets for strain measurements.

meant to verify variation of load-bearing capacity of beams with mass loss of steel. It also represents a conservative approach where the time of first appearance of visible corrosion cracks is used as a criterion of end-of-service life of corrosion-affected RC structures.

Steel corrosion was limited to tensile steel bars and only the middle part of bars with a span of 700 mm was corroded (Figs. 2 and 3). At the end of serviceability testing, residual load-bearing capacities of beams and mass losses of steel were measured and are discussed in detail in Malumbela et al. [15]. Their results will only be mentioned here to corroborate discussions in the paper.

Rather than directly measuring crack widths as done by many other researchers discussed earlier, in this research transverse strains across corrosion cracks were measured instead. As shown in Fig. 3, seven sections at spacings of 100 mm and limited to the corrosion region were monitored for transverse strains on tensile faces of beams. This was done using a demec gauge with a gauge length of 100 mm and a range of ±10 to ±5000 micro strains. A minimum strain of 10 micro strains recorded from the gauge is therefore equivalent to a crack widening of 0.001 mm. Vertical strains on side faces were also measured at seven sections that were directly opposite the measuring sections on tensile faces. During accelerated corrosion, strains were measured before and after each wetting cycle. For the first set of beams tested in the research, the accelerated corrosion set-up was such that vertical strains near corroding steel bars could not be measured. The change of the set-up to allow for them to be monitored was primarily carried out to assess the nature of strains on uncracked side faces of beams. As was discussed in Malumbela et al. [16], this change was equally important in assessing the effectiveness of FRP strengthening schemes used in the research to control the rate of corrosion crack widening. It should be mentioned that despite the change in corrosion set-up, it was not possible to measure vertical strains on all side faces of beams. A number of beams under nominally similar conditions were tested.

4. Results

4.1. Corrosion crack patterns

Table 1 gives corrosion crack patterns that were exhibited by beams in this research namely; crack pattern A, crack pattern B and crack pattern C. Similar to results from Ballim et al. [1,2], El Maaddawy et al. [12] and Zhang et al. [5,13,14], these results indicate that it is difficult to associate corrosion crack patterns with level of sustained load.

In crack pattern A, a single crack that propagated parallel to corroded steel bars was observed on the tensile face of a beam where corrosion agents were drawn into the concrete. As shown by Table 1 and Fig. 1, only one beam corroded to a theoretical mass loss of steel of 10% (beam 16) and all lightly corroded beams (beams 8, 11, and 12) from beams tested in this research exhibited this crack pattern.

In crack pattern B, a beam initially cracked on its tensile face as in crack pattern A. However, as corrosion continued, another crack was observed on one side face of the beam whilst the other side face remained uncracked. The crack on the side face of the beam was at the level of the corroding tensile reinforcement and

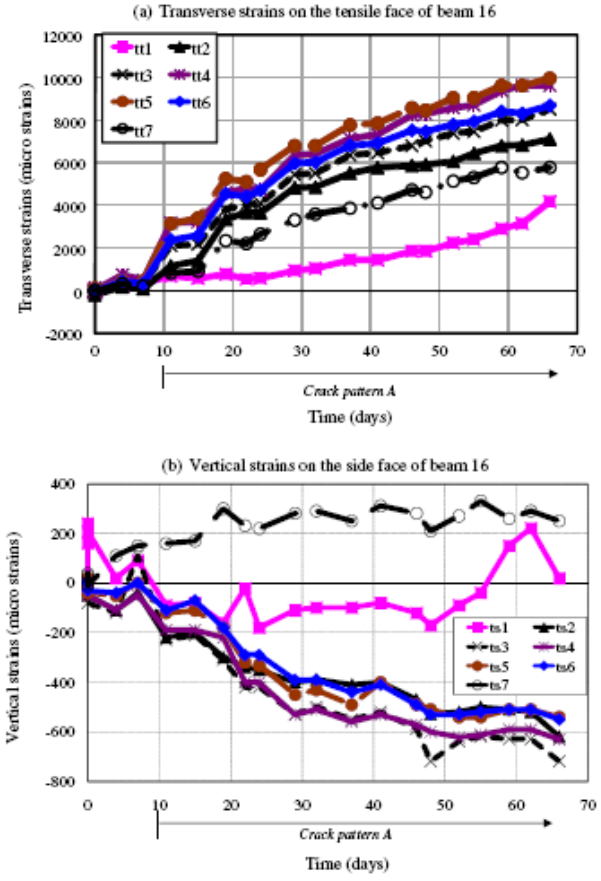

Fig. 4. Transverse and vertical strains for crack pattern A.

propagated (parallel to the bars) to a distance of about 150 mm beyond the ends of the corrosion region. The majority of beams in this research exhibited this crack pattern as indicated by Table 1. The times at which crack patterns in various beams changed from crack pattern A to crack pattern B were however, different and ranged from about 19 days to about 50 days.

In crack pattern C, a beam initially cracked on its tensile face (crack pattern A) followed by a crack on one side face (to give crack pattern B) and finally cracked on the other side face as corrosion continued. It is important to mention that cracks on side faces in crack pattern C were observed at different times. For beam 17, a crack on one side face was observed after 25 days and on the other, after 33 days of testing.

The above discussed crack patterns were the main patterns that were observed. In a few beams, side faces that were considered uncracked actually had small isolated corrosion cracks which probably indicated a change between crack patterns. As already mentioned, change in crack patterns as steel corrosion progressed was also reported by El Maaddawy and Soudki [8]. The primary difference between crack patterns obtained here to those found by other researchers is that they at times found multiple cracks on tensile faces of beams that propagated along positions of each reinforcing bar [6,8,11]. This is probably because they used larger spacing between bars. For example, El Maaddawy and Soudki [8] used bar spacing of about 80 mm whilst in this research, a clear spacing of 18 mm between bars was used. Both bar spacings are practical and accepted in various design codes such as the South African National Standard [17].

It was found here and also by other researchers [8,11,12] that even for nominally identical specimens, it is difficult to predict the type of crack pattern that each specimen will exhibit. As already mentioned, the majority of specimens here and elsewhere [8,12], firstly exhibited crack pattern A at the early corrosion stages (such as beams 8, 11, and 12) followed by crack pattern B as corrosion was continued.

4.2. Widening of corrosion cracks in crack pattern A

Transverse and vertical strains in beam 16 (with crack pattern A) are shown in Fig. 4. It is clear from the figure that large transverse tensile strains were recorded on the tensile face of the beam. However, vertical strains on its side face (ts1 and ts7 aside) were largely contractional. Vertical strains at ts1 and ts7 can be attributed to location of discrete corrosion cracks. The figure also shows that each measuring point along the tensile face of the beam demonstrated a near-constant rate of increase of transverse tensile

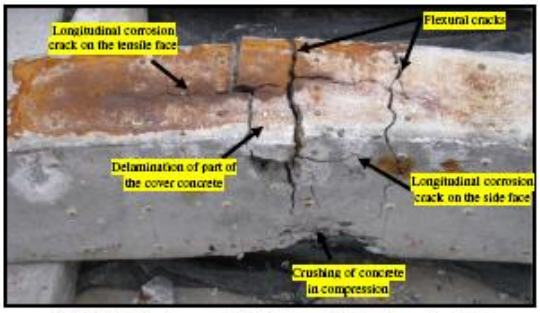

NB! Tensile face of a corroded RC beam at failure (beam inverted)

Fig. 5. Failure mode of beam 4 (crack pattern B).

strains during testing. This implies that the width of corrosion cracks on the tensile face of the beam widened at a near-constant rate as steel corrosion continued. To predict accurately the rate of widening of corrosion cracks, it is important to understand the behaviour of the cover concrete due to steel corrosion.

To help explain influence of crack patterns on deformation of cover concrete, ultimate failure modes of beams 4, 9, and 17 are shown here as Figs. 5 and 6. As shown in Table 1, beam 4 exhibited crack pattern B while beams 9 and 17 exhibited crack pattern C. It is clear from Fig. 6 that combined flexural cracks due to applied loads and longitudinal cracks from steel corrosion detached the cover concrete of beams 9 and 17 from the parent concrete. In beam 4, delamination of the cover concrete was only observed on sections of the corroded length where the beam exhibited side cracks (Fig. 5). For the cover concrete to delaminate due to flexural cracks and corrosion cracks, then certainly it wasn't attached to the parent concrete beam. It is therefore reasonable to assume that for crack pattern A, the majority of the cover concrete was attached to the parent concrete beam. However, surely for a crack that is limited to the cover concrete to widen as indicated by Fig. 4a, some sections of the cover concrete must be detached from the parent concrete beam to permit slippage between them.

It is logical that during corrosion, first sections of the cover concrete to be detached from the parent concrete are around corroding bars. This is because in those regions, the cover concrete will be pushed outwards to allow for deposit of voluminous corrosion products. Fig. 7 shows a picture of exposed corroded area when beam 11 (crack pattern A) was opened for repair. From the figure, corrosion products were largely observed within the area bound by corroding steel bars with little products on the side cover concrete.

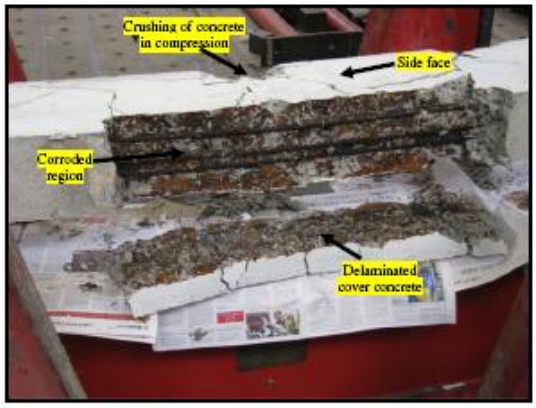

(a) Tensile face of a corroded RC beam (beam 9 lying on the side face)

(b) Side view of a corroded RC beam (beam 17) at failure

Fig. 6. Failure mode of beams 9 and 17 (crack pattern C).

In this paper this area (shown in Fig. 7) will be named the corrosion region. It is reasonable to assume that for crack pattern A, the cover concrete is only detached from the parent concrete within the corrosion region. The side cover concrete (shown in Fig. 7) remains fully-attached to the parent concrete beam.

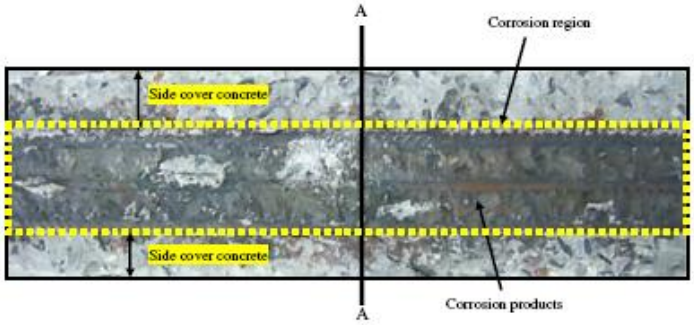

Fig. 7. Distribution of corrosion products in a beam with crack pattern A.

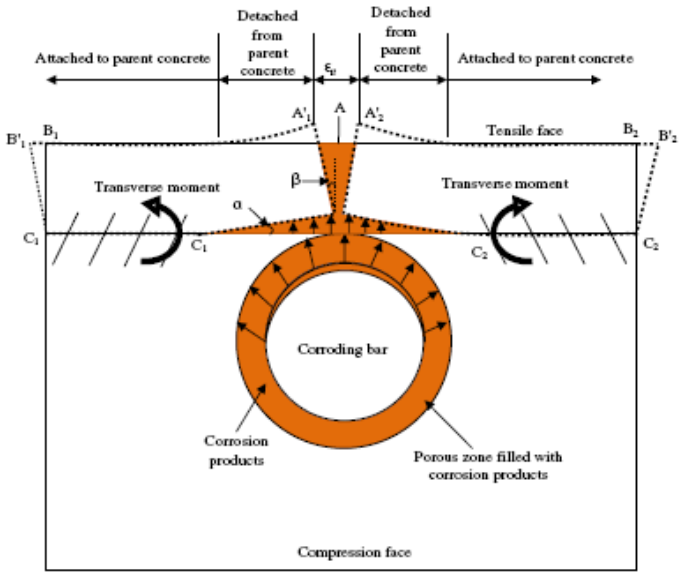

Fig. 8. Cross-section of a corroding beam with crack pattern A.

From the above-discussion, a cross-section through A–A (prior to removing cover concrete) of Fig. 7 can be schematically represented by Fig. 8. For clarity, only one corroding bar, instead of three used in this research, is shown in the figure. As the figure shows, to allow for deposit of corrosion products around the bar, the cover concrete was pushed outwards. Since it was fixed on the sides, pressure from steel corrosion induced internal transverse moments where it was fixed. Bear in mind that before corrosion products apply pressure on cover concrete, they must completely fill the porous zone between steel and concrete [18,19].

It should be mentioned that prior to cover cracking, targets on tensile faces of beams recorded actual transverse tensile strains on fibres of the concrete. Vertical strains on side faces of the beam were therefore due to Poisson's effects. This can be confirmed by ratios between strains reported in Malumbela et al. [19,20]. However, after cracking, rather than recording strains on fibres of the concrete, targets on tensile faces recorded widening of corrosion cracks. This is because they were purposely placed across the cracks. Vertical strains on side faces were therefore, not a Poisson's effect of recorded transverse strains on tensile faces. Moreover, values of vertical strains recorded on side faces of beams were too large to have been due to Poisson's effects of actual strains on other faces. For example, for a compressive strain of 600 micro strains on concrete to be due to Poisson's effects, the corresponding tensile strain should be about 3000 micro strains which is not possible for uncracked concrete. Therefore, similar to targets on tensile faces, targets on vertical faces of beams recorded translation of the cover concrete rather than actual strains on fibres of the concrete. The word 'translation' is used here to avoid mistaking it for deformation which is a direct result of stresses on the concrete.

From Fig. 4, widths of corrosion cracks on tensile faces of beams with crack pattern A recorded as transverse tensile strains (Fig. 4a), is because point A in Fig. 8 shifted to points A'. If points B_1 and B_2 were to be stationary or fixed, then the cover concrete was supposed to significantly compress to allow for the A–A' movement. Considering the width of corrosion cracks that were recorded in beam 17 (up to 1 mm) and half the width of the beam (76.5 mm), this is not possible. Therefore, point B had to move to points B'. The movement B-B' was possible because fixity of the cover concrete discussed earlier was along C–C whilst point B was free. It is this movement that is attributed to the large contractional vertical strains recorded on side faces of beams. Certainly vertical stresses applied on the cover concrete by corrosion products shown in Fig. 8 were resisted by the tensile strength of concrete along C–C. As corrosion continued, applied stresses increased so that section C–C finally cracked to give crack pattern B.

4.3. Widening of corrosion cracks in crack pattern B

Fig. 9 shows transverse strains on tensile faces and vertical strains on side faces of beams that exhibited crack pattern B. As mentioned earlier, beams 14 and 15 are some of beams that had to be tested under nominally similar conditions because it was not possible to measure vertical strains on all sides. The figure shows that under this crack pattern, tensile strains (transverse and vertical) were recorded on faces of beams that had corrosion cracks (Fig. 9a, c, and d) whilst contractional strains were recorded on uncracked side faces (Fig. 9b). Fig. 9c and d shows that before recording vertical tensile strains on side faces of beams, rates of increase of transverse tensile strains on the tensile face of beams were nearly constant and about the same as in beams with crack pattern A. This is expected since at that stage, they were under the category of crack pattern A. Interestingly, when vertical strains were recorded on side faces of beams such as after 19 days for beam 15, rates of increase of corresponding transverse tensile strains on tensile faces decreased. However, rates of increase of vertical tensile strains on the (now) cracked side faces of beams were nearly constant through the entire testing period as shown in Fig. 9d. In beam 14, cracks on the side face (which was not monitored) appeared after 20 days. Similar to beam 15, rates of increase of transverse strains on the tensile face of the beam decreased. Interestingly, contractional vertical strains on the uncracked side face of the beam were not affected by cracking of the other side face of the beam. This implies that a longitudinal crack on the

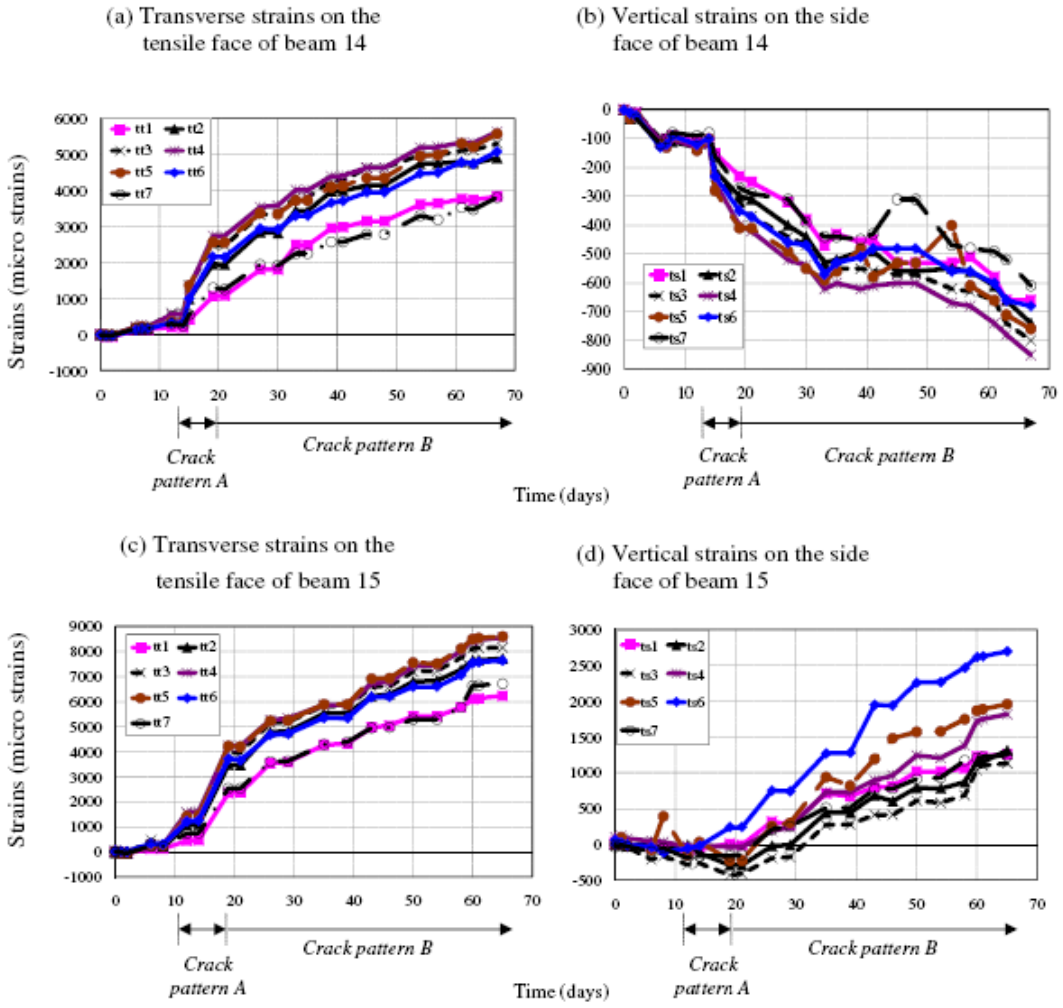

NB! Crack width (mm) = tensile strains (micro strains) * 0.0001

Fig. 9. Transverse and vertical strains for crack pattern B.

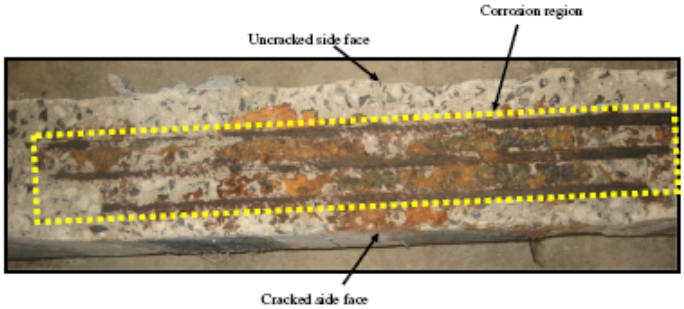

Fig. 10. Distribution of corrosion products in crack pattern B.

tensile face of the beam resulted in the divided parts of the cover concrete behaving independent of each other.

From the behaviour of the cover concrete in Fig. 8, vertical tensile strains on side faces of beams can only be recorded when section C–C is cracked. This would imply that within the corroded length of the beam, the part of the cover concrete with a corresponding cracked side face was completely detached from the parent concrete beam. In corroboration, Fig. 6 showed delamination of part of the cover concrete that exhibited corrosion cracks on the tensile face as well as on the side face. Similar to crack pattern A, the distribution of corrosion products (Fig. 10) can also be used to assess sections of the cover concrete that were attached or detached from the parent concrete beam. As previously mentioned, where they are observed, then the cover concrete was pushed outwards (detached from the parent concrete) to allow for them to be deposited. Fig. 10 clearly shows detached sections in crack pattern B to have been the corrosion region (as in crack pattern A) as well as the side cover concrete which corresponded to a cracked side face.

A cross-section of a corroding beam with crack pattern B can therefore be schematically presented by Fig. 11. As shown in the figure, corrosion products pushed part of the cover concrete with a cracked side face (designated by a subscript 1) directly upwards. The other part behaved like those in crack pattern A. Since point A'_1 no longer moved in the transverse direction but rather in the vertical direction, transverse strains recorded on the tensile face of the beam were only due to the movement of $A–A'_2$. Expectedly, Fig. 9c shows that rates of increase of transverse strains on the tensile face of beam 15 decreased when vertical tensile strains were recorded on the side face. Moreover, part of the cover concrete with a corresponding uncracked side face (designated by subscript 2) continued to exhibit large vertical contractional strains to suggest the $A–A'_2$ movement (Figs. 9b and 11).

4.4. Widening of corrosion cracks in crack pattern C

As shown in Fig. 12, the variation of transverse strains on the tensile face and vertical strains on the side face found in crack pattern C was initially similar to that recorded in crack pattern A followed by that in crack pattern B. Contrary to crack patterns A and B, when both side faces of the beam cracked in crack pattern C (33 days for beam 17), transverse tensile strains on the tensile face of the beam stabilised and ceased to increase despite continued corrosion. After cracking, the rate of increase of vertical tensile strains on the side face of the beam however, remained near constant as shown in Fig. 12b.

It was pointed out under crack pattern B that part of the cover concrete which exhibited cracks on the tensile face as well as on the side face was detached from the parent concrete beam. In crack pattern C here, all side faces were cracked. This implies that over the corroded region, as well as on the side cover concrete, the entire cover concrete was detached from the parent concrete beam. This was corroborated by delamination of the entire cover concrete when beams 9 and 17 (with crack pattern C) were tested to failure (Fig. 6). Corrosion products in Fig. 6a were uniformly distributed around the corroded area as well as on the side cover concrete. This again suggests that within the corrosion region, the cover concrete was completely detached from the parent concrete. A cross-section of the beam on the corrosion region is shown in Fig. 13. The figure shows that corrosion products pushed A'_1 and A'_2 upwards. As indicated by transverse strains on the tensile face, there was little transverse movement of A–A'. However, vertical strains on the two side faces of the beam increased. Note that here, the cover concrete was attached to the parent concrete only at the ends of the corrosion region.

4.5. Discussion on rate of widening of corrosion cracks

As previously mentioned, prior to a change of crack patterns, the majority of beams exhibited a similar rate of widening of corrosion cracks. This is confirmed using Fig. 14 which shows the variation of transverse tensile strains on tensile faces of beams after three wetting cycles or 12 days of impressed current density. During this period, all beams shown in the figure exhibited crack pattern A. Exception was beam 9, 10, and 20. Beams 9 and 10 had maximum crack widths on the side face which, as pointed out

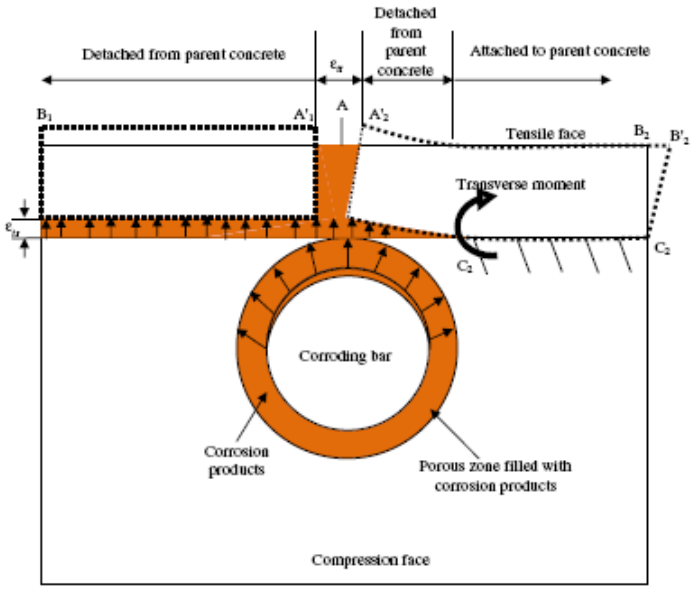

Fig. 11. Cross-section of a corroding beam with crack pattern B.

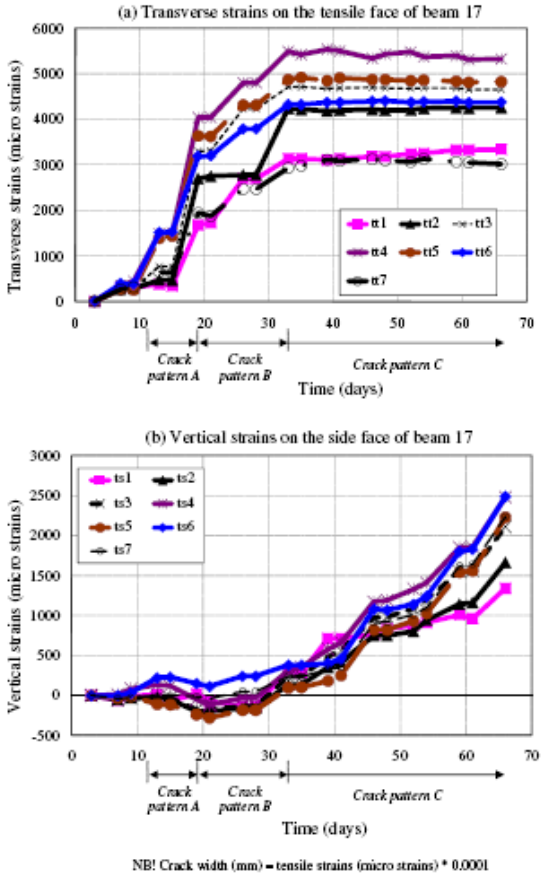

Fig. 12. Transverse and vertical strains for crack pattern C.

earlier, the initial experimental set-up could not monitor. Beam 20 had maximum crack widths on the side face which also could not be monitored. It however, showed interesting behaviour after repair which will be discussed in other publications.

The period shown in Fig. 14 corresponded to a total of 24 days for beams with four-day drying cycles and 18 days for those with two-day drying cycles. The position along the beam shown in the figure was measured from the current input side of the beam to the current output side. 'Zero' in the figure therefore indicates the edge of the corrosion region on the current input side whilst 700 mm indicates the edge of the region on the current output side. It is clear from the figure that after three wetting cycles, maximum crack widths from various beams ranged from 0.35 to 0.55 mm.

At the end of accelerated corrosion (64 days for beams with two-day drying cycles and 80 days for those with four-day drying cycles), beam 16 (still with crack pattern A) had a maximum crack width of 1 mm compared to 0.54 mm in beam 17 (now with crack pattern C). Moreover, the widest crack in beam 17 was dormant whilst cracks on the side face of the beam, which were actively-widening, had a maximum width of 0.25 mm (Fig. 12). In contrast, the crack width of 1 mm on the tensile face of beam 16 was still actively-widening. The obvious implication is that end-of-service life that is based on the criterion of maximum corrosion crack width of 1 mm is likely to suggest repair of RC structures with crack pattern A prior to those with crack pattern C.

It should be pointed out that Figs. 4, 9 and 12 are not always possible to draw for in-service structures because practitioners often measure corrosion crack widths on corroded RC structures at discrete times. They then use maximum corrosion crack widths to predict levels of steel corrosion as well as to assess if there is need for repair [1,2,6,12]. To understand the implication of this, Fig. 15 shows maximum tensile strains (or crack widths) at the end of accelerated corrosion for various beams in this research.

Only transverse tensile strains on tensile faces of beams are shown in Fig. 15 because except for beams 9, 10, and 20 (already discussed), they still exhibited maximum crack widths. Beam 17, despite having a dormant crack on the tensile face for nearly half the total time of accelerated corrosion testing, also exhibited maximum cracks on the tensile face. If steel corrosion was to be continued, it is expected however, that maximum crack widths in beam 17 would belong with the side face as opposed to the tensile face. Interestingly, other beams that exhibited crack pattern B and had maximum cracks on the tensile face such as beams 6, 7, and 14 had comparable crack widths as beam 17. This points out to the complexity of the rate of widening of corrosion cracks, especially at larger crack widths.

Contrary to maximum crack widths after three wetting cycles discussed earlier, maximum crack widths at the end of corrosion were very different. Owing to varying times at which different corrosion crack patterns were observed on beams (indicated by Figs. 4, 9 and 12) and since rates of widening of corrosion cracks were closely related to crack patterns, beams were expected to show these varying corrosion crack widths. As discussed earlier, the figure shows that a beam with crack pattern A (beam 16) had widest corrosion cracks. Unfortunately, narrowest cracks belonged with a beam with crack pattern B (beam 7).

The overall implication from Fig. 15 is that for wider cracks, it is difficult to provide a deterministic value for maximum crack widths of corroding beams. Results on crack pattern A are really not conclusive since it was only found in one heavily corroded beam. Previous discussion however, indicated that as corrosion progresses, it changes to crack pattern B. Since this research and others [8,12] did not find a definite level of steel corrosion at which crack pattern A changed to crack pattern B, there is large variation of crack widths in crack pattern B. It is therefore difficult to predict accurately crack widths in this crack pattern. However, crack pattern C offers the most challenge because unless corrosion cracks are continuously monitored as in Fig. 12, it is difficult to predict accurately when it occurred.

Discussions of results from Alonso [7] and from Cabrera [11], pointed out that crack pattern C (as in this research) only occurs where the cover depth of exterior bars to the tensile face is equal to their cover depth to the side face. Where they are different, RC specimens exhibit crack pattern A. Zhang et al. [13] recommends that where a corroding bar causes two cracks on adjacent faces of a RC structure, an equivalent crack width should be taken as the sum of the two cracks. Their assertions will be confirmed here using deformation of cover concrete shown in Fig. 8.

As previously noted, it is reasonable to assume little deformations of the cover concrete under crack pattern A so that crack widths on the tensile face were mainly due to its translation (movement without bending). Angles α and β shown in Fig. 8 were therefore nearly equal. This section of the cover concrete is further illustrated using Fig. 16. If distances 'a' and 'b' in Fig. 16 are equal and the cover concrete only rotates but does not deform then $\Delta_{vertical}$ equals $\Delta_{transverse}$. The implication of this is that vertical movement of the cover concrete (which gave vertical tensile strains on the side face if C–C was free as in Fig. 11) was equal to $A-A'_2$ movement. It follows then that the rate of widening of

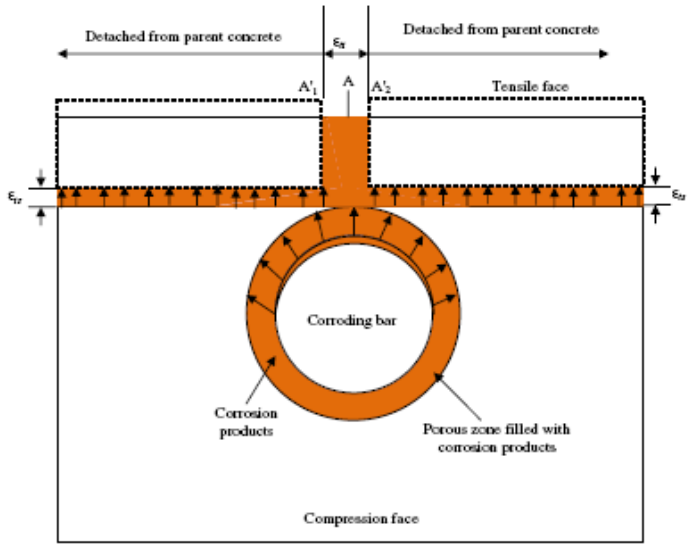

Fig. 13. Cross-section of a corroding beam with crack pattern C.

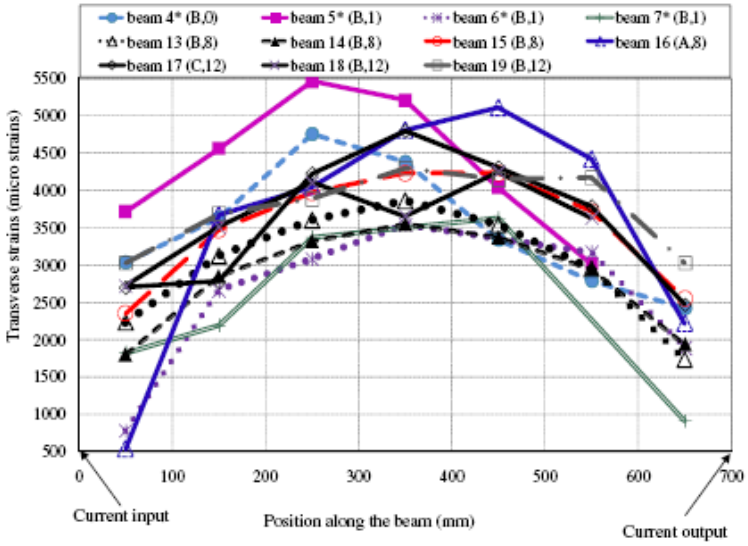

NB! Crack width (mm) = tensile strains (micro strains) * 0.0001

Designation: * = corroded using four-day drying cycles; letter in brackets indicates the crack pattern at the end of accelerated corrosion; and a number in brackets indicates the level of sustained load during accelerated corrosion.

Fig. 14. Transverse strains after 12 days of accelerated corrosion.

corrosion cracks on the side face of a RC beam with crack pattern C should be half its rate of widening on the tensile face if it exhibits crack pattern A. To confirm this notion, for the first 20 days, the rate of widening of corrosion cracks in beam 17 (then with crack pattern A) was 19 μm/day. When it exhibited crack pattern C, the rate of widening of cracks on the side face was 8.1 μm/day. If this is implemented on crack widths in beam 17, it gives crack widths that are similar to those found under crack pattern B.

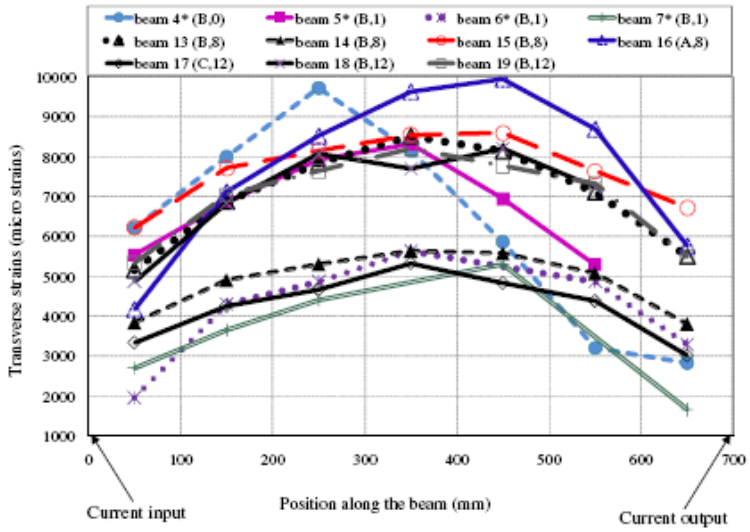

NB! Crack width (mm) = tensile strains (micro strains) * 0.0001

Designation: * = corroded using four-day drying cycles; letter in brackets indicates the crack pattern; and a number in brackets indicates the level of sustained load during accelerated corrosion.

Fig. 15. Transverse strains at the end of accelerated corrosion.

Another interesting feature about Figs. 14 and 15 is that corrosion crack widths on beams varied longitudinally along the corroded region with maximum cracks experienced at the centre of the corrosion region. Smaller cracks were found at the ends of the region. This can be attributed to an increase in transverse stiffness of beams by shear stirrups that were only placed within the shear span (Fig. 2). If they were uniformly placed along the beam, maximum corrosion crack widths would probably be at random as found by Zhang et al. [5,13,14]. Results from El Maaddawy et al. [12] where fewer stirrups were placed within the corroded region also showed maximum corrosion crack widths at the centre of the corrosion region. On the other hand, Ballim et al. [1,2] found maximum corrosion crack widths at beam ends most probably because they had fewer stirrups there. Note that it is a common practice to reduce shear stirrups around constant moment regions. This research therefore presents the worst scenario where the corrosion region does not have shear stirrups. Another argument to this behaviour as presented by François and Arliguie [21] is that it is the loss in adhesion at the steel–concrete interface that causes large crack widths. This adhesion is of good quality around stirrups so that minimum crack widths are found there. Further research to confirm these arguments is necessary.

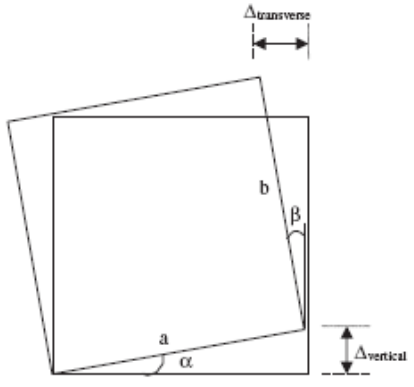

Fig. 16. Schematic of mechanism of widening of corrosion cracks.

5. Relation between crack widths and mass loss of steel

Fig. 17 shows the variation of loss of steel in beams as previously discussed by Malumbela et al. [15]. From the figure and based on the duration of the accelerated corrosion, it can be shown that mass loss of steel under two-day drying cycles ranged from 1.1 to 1.68 g/day/m of bar length. In relation to maximum crack widths in Fig. 14 (below 0.6 mm), it can be shown that 1% mass loss of steel corresponded to maximum crack widths between 0.14 and 0.22 mm. These relations give larger rates of widening of corrosion cracks than those presented earlier from previous researchers. They contended that 1% mass loss of steel corresponds to crack widths between 0.03 and 0.14 mm. Note that previous researchers monitored crack widths at the end of corrosion. Therefore, there is likelihood that the rates of widening of corrosion cracks that they provided included a change of crack patterns. However, Fig. 14 is only when beams exhibited crack pattern A. Should that be true then relations provided by previous researchers may overestimate service life of corroding RC structures.

As already mentioned, above relations were based on mass losses of steel with two-day drying cycles. This is because Malumbela et al. [15] pointed out that long drying cycles caused larger losses of steel because they allowed more drying of the corrosion

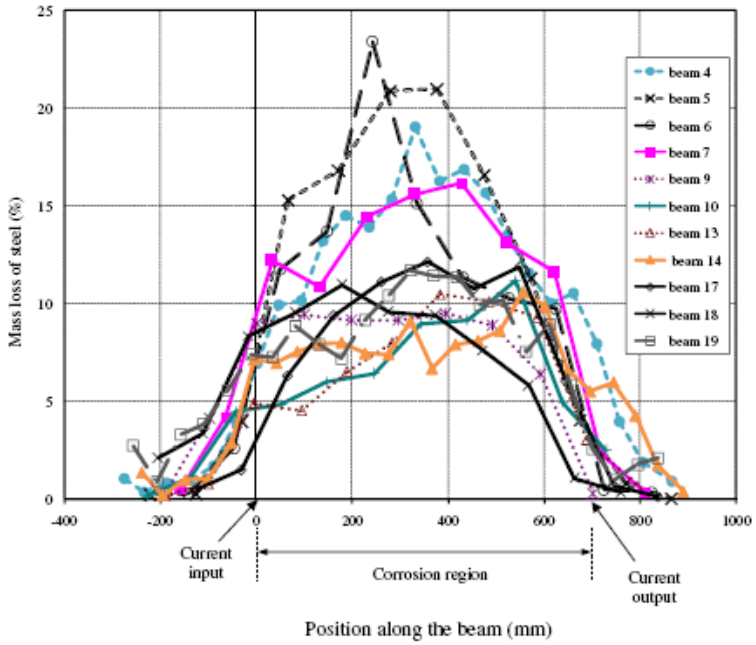

Fig. 17. Variation of mass loss of bars along the beam [15].

region. Influence of dryness of concrete on rate of steel corrosion was also found by Torres-Acosta et al. [10]. At the early corrosion stages such as in Fig. 14 as well as prior to cover cracking, the influence of long drying cycles on the rate of steel corrosion was not yet expected. However, for in-service structures where it would take tens of years to reach a crack width of 0.6 mm, different relations are expected. They are discussed using crack widths at the end of steel corrosion.

Probably the most important information from Figs. 15 and 17 is that despite having larger rates of steel corrosion, beams with four-day drying cycles (beams 4–7) did not necessarily have the widest corrosion cracks. For example, beam 6 had the largest maximum mass loss of steel (Fig. 17) and it was within a group of beams (beam 6, 7, 14, and 17) that exhibited the narrowest corrosion cracks (Fig. 15). Note that large rates of corrosion on beams with four-day drying cycles was attributed to longer drying periods allowing for more drying of the corrosion region and hence resulting in formation of less voluminous products such as haematite [15]. This most likely allowed for more corrosion agents to reach the steel. It also left more space which permitted deposit of additional corrosion products without applying excessive stresses on the cover concrete. However, other beams with four-day drying cycles, especially beam 4, exhibited maximum corrosion crack widths that were comparable with those in beam 16. This was despite beam 4 having crack pattern B. Contrary to other beams where crack pattern B was observed after about 20 days of corrosion, in beam 4 it was observed after 50 days. Therefore, when rates of widening of corrosion cracks on its tensile face were reduced by a change of crack patterns, it had already extensively widened. To confirm this notion, after three wetting cycles, beams 5 and, interestingly, 17 had wider cracks than beam 4.

Figs. 15 and 17 imply that a corroding RC beam with a maximum crack width of 0.54 mm (crack pattern B) can have mass losses of steel ranging from 7.9 (two-day drying cycles) to 23.4% (four-day drying cycles). A similar range of mass loss of steel can be obtained by a beam with a crack width of 1 mm (crack pattern A). Therefore, according to crack widths limits in [22], one beam may be recommended for repair when it has a mass loss of steel of 7.9% and another considered safe when its mass loss of steel is 23.4%. A conservative approach is to assume that a beam with the smallest crack width has the largest mass loss of steel. In fact, this was the case for beam 6. Under this approach, a crack width of 0.54 mm corresponded to a mass loss of steel of 23.4%. Assuming a constant rate of widening of corrosion cracks as well as a constant rate of loss of steel, then 1% maximum mass loss of steel corresponded to a maximum crack width of 0.02 mm.

Note that the above relation follows the recommendation that maximum crack widths in crack pattern C are the sum of two adjacent cracks as discussed using Figs. 11 and 16. If it is not followed, then practitioners are likely to underestimate the level of steel corrosion in RC structures that have this crack pattern. For example, if repair was to be carried out at a crack width of 1 mm, then beam 17 was only going to exhibit it on the side face after about 150 days. If the beam had the maximum rate of steel corrosion found in this research, then at repair, it was expected to have a mass loss of steel of about 53%.

6. Conclusions

1. After cracking of the cover concrete and with corrosion cracks below 0.6 mm, it was found that various beams exhibited a near-similar rate of widening of corrosion cracks. It was therefore concluded that service life of corroding RC structures that is based on corrosion crack widths below 0.6 mm such as a limit of 0.3 mm by DuraCrete Final Technical Report [22] is unlikely to be significantly variable between identical structures. For corrosion crack widths greater than 0.6 mm, it was found that

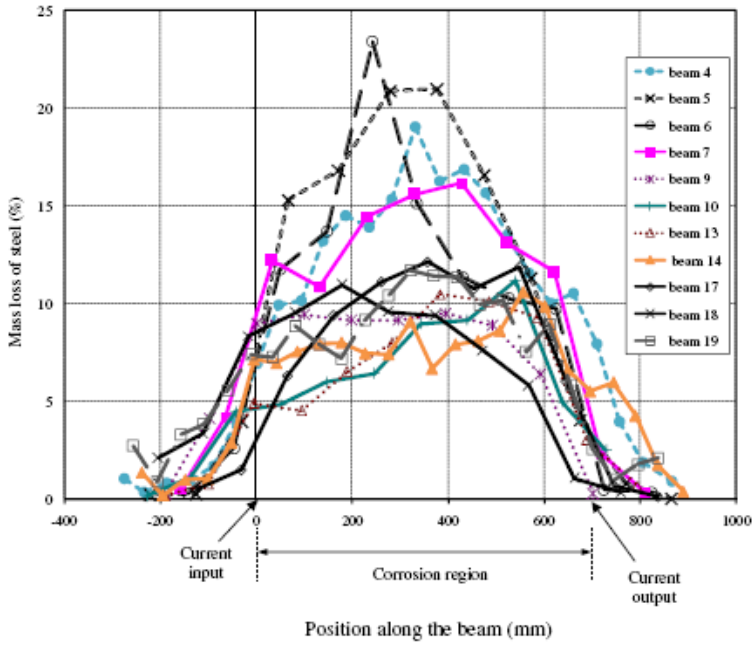

Fig. 17. Variation of mass loss of bars along the beam [15].

region. Influence of dryness of concrete on rate of steel corrosion was also found by Torres-Acosta et al. [10]. At the early corrosion stages such as in Fig. 14 as well as prior to cover cracking, the influence of long drying cycles on the rate of steel corrosion was not yet expected. However, for in-service structures where it would take tens of years to reach a crack width of 0.6 mm, different relations are expected. They are discussed using crack widths at the end of steel corrosion.

Probably the most important information from Figs. 15 and 17 is that despite having larger rates of steel corrosion, beams with four-day drying cycles (beams 4–7) did not necessarily have the widest corrosion cracks. For example, beam 6 had the largest maximum mass loss of steel (Fig. 17) and it was within a group of beams (beam 6, 7, 14, and 17) that exhibited the narrowest corrosion cracks (Fig. 15). Note that large rates of corrosion on beams with four-day drying cycles was attributed to longer drying periods allowing for more drying of the corrosion region and hence resulting in formation of less voluminous products such as haematite [15]. This most likely allowed for more corrosion agents to reach the steel. It also left more space which permitted deposit of additional corrosion products without applying excessive stresses on the cover concrete. However, other beams with four-day drying cycles, especially beam 4, exhibited maximum corrosion crack widths that were comparable with those in beam 16. This was despite beam 4 having crack pattern B. Contrary to other beams where crack pattern B was observed after about 20 days of corrosion, in beam 4 it was observed after 50 days. Therefore, when rates of widening of corrosion cracks on its tensile face were reduced by a change of crack patterns, it had already extensively widened. To confirm this notion, after three wetting cycles, beams 5 and, interestingly, 17 had wider cracks than beam 4.

Figs. 15 and 17 imply that a corroding RC beam with a maximum crack width of 0.54 mm (crack pattern B) can have mass losses of steel ranging from 7.9 (two-day drying cycles) to 23.4% (four-day drying cycles). A similar range of mass loss of steel can be obtained by a beam with a crack width of 1 mm (crack pattern A). Therefore, according to crack widths limits in [22], one beam may be recommended for repair when it has a mass loss of steel of 7.9% and another considered safe when its mass loss of steel is 23.4%. A conservative approach is to assume that a beam with the smallest crack width has the largest mass loss of steel. In fact, this was the case for beam 6. Under this approach, a crack width of 0.54 mm corresponded to a mass loss of steel of 23.4%. Assuming a constant rate of widening of corrosion cracks as well as a constant rate of loss of steel, then 1% maximum mass loss of steel corresponded to a maximum crack width of 0.02 mm.

Note that the above relation follows the recommendation that maximum crack widths in crack pattern C are the sum of two adjacent cracks as discussed using Figs. 11 and 16. If it is not followed, then practitioners are likely to underestimate the level of steel corrosion in RC structures that have this crack pattern. For example, if repair was to be carried out at a crack width of 1 mm, then beam 17 was only going to exhibit it on the side face after about 150 days. If the beam had the maximum rate of steel corrosion found in this research, then at repair, it was expected to have a mass loss of steel of about 53%.

6. Conclusions

1. After cracking of the cover concrete and with corrosion cracks below 0.6 mm, it was found that various beams exhibited a near-similar rate of widening of corrosion cracks. It was therefore concluded that service life of corroding RC structures that is based on corrosion crack widths below 0.6 mm such as a limit of 0.3 mm by DuraCrete Final Technical Report [22] is unlikely to be significantly variable between identical structures. For corrosion crack widths greater than 0.6 mm, it was found that

beams exhibited three different types of crack patterns; crack pattern A, B, and C, with crack pattern A having the largest rate of widening of corrosion cracks followed by crack pattern B. Based on the rate of widening of corrosion cracks from the various crack patterns, it was concluded that service life of corroding RC structures that is based on the criterion of corrosion crack widths above 0.6 mm such as a limit of 1 mm [22], is likely to prescribe repairs of structures that exhibit crack pattern A before those that exhibit crack patterns B or C.

2. If steel corrosion entails wetting and drying of specimens with salt solution, longer drying cycles yield larger rates of steel corrosion. On the contrary, this paper showed that patterns of corrosion cracks as well as rate of widening of the cracks in each pattern were independent of the duration of drying cycles. It was therefore concluded that the worst scenario to structural engineers and asset managers was when a structure had longer drying cycles (larger corrosion rates) and exhibited crack pattern C (low rate of widening of corrosion cracks). Without a clear understanding of the relations between; the pattern of corrosion cracks; the rate of widening of the cracks; and the rate of steel corrosion, relations between maximum corrosion crack widths and maximum loss of steel area due to corrosion are likely to prescribe repairs of structures that exhibit crack pattern C (worse if they have longer drying cycles) at dangerous levels of steel corrosion.
3. Based on the variation of corrosion crack widths, it was recommended that for beams that exhibit cracks on the tensile face as well as on the near side face (crack pattern C), the maximum crack width should be taken as the sum of the maximum cracks from each face of the beam. If the recommendations in this research are followed then a maximum mass loss of steel of 1% corresponded to a maximum corrosion crack width of 0.02 mm.
4. It is important to mention that results in this paper may not be representative of actual structural damage where corrosion is natural. They therefore need to be verified with results under natural steel corrosion. It is however, reasonable to say that service life of RC structures based on criterion of corrosion crack widths should take into account the crack pattern.

Acknowledgement

The support of the Concrete Materials & Structural Integrity Research Group (CSIRG) at the University of Cape Town is greatly acknowledged.

References

[1] Ballim Y, Reid JC, Kemp AR. Deflection of RC beams under simultaneous load and steel corrosion. Mag Conc Res 2001;53(3):171–81.
[2] Ballim Y, Reid JC. Reinforcement corrosion and deflection of RC beams – an experimental critique of current test methods. Cem Conc Compos 2003;25:625–32.
[3] Yoon S, Wang K, Weiss J, Shah S. Interaction between loading, corrosion, and serviceability of reinforced concrete. ACI Mater J 2000;97(6):637–44.
[4] Malumbela G, Moyo P, Alexander MG. Behaviour of RC beams corroded under sustained service loads. Constr Build Mater 2009;23:3346–51.
[5] Zhang R, Castel A, François R. Serviceability limit state criteria based on steel–concrete bond loss for corroded reinforced concrete in chloride environment. Mater Struct 2008. doi:10.1617/s11527-008-9460-.
[6] Torres-Acosta AA, Martinez-Madrid M. Residual life of corroding reinforced concrete structures in marine environment. J Mater Civil Eng 2003;15(4):344–53.
[7] Alonso C, Andrade C, Rodriguez J, Diez JM. Factors controlling cracking of concrete affected by reinforcement corrosion. Mater Struct 1998;31:435–41.
[8] El Maaddawy T, Soudki K. Effectiveness of impressed current technique to simulate corrosion of steel reinforcement in concrete. J Mater Civil Eng 2003;15(1):41–7.
[9] Badawi M, Soudki K. Control of corrosion-induced damage in reinforced concrete beams using carbon fiber-reinforced polymer laminates. J Compos Constr 2005;9(2):195–201.
[10] Torres-Acosta AA, Navarro-Gutierrez S, Terán-Guillén J. Residual flexure capacity of corroded reinforced concrete beams. Eng Struct 2007;29:1145–52.
[11] Cabrera JG. Deterioration of concrete due to reinforcement steel corrosion. Cem Concr Compos 1996;18:47–59.
[12] El Maaddawy T, Soudki K, Topper T. Long-term performance of corrosion-damaged reinforced concrete beams. ACI Struct J 2005;102(5):649–56.
[13] Zhang R, Castel A, François R. Concrete cover cracking with reinforcement corrosion of RC beam during chloride-induced corrosion process. Cem Concr Res 2010;40:415–25.
[14] Zhang R, Castel A, François R. The corrosion pattern of reinforcement and its influence on serviceability of reinforced concrete members in chloride environment. Cem Concr Res 2009;39:1077–86.
[15] Malumbela G, Alexander MG, Moyo P. Variation of steel loss and its effect on flexural capacity of RC beams corroded and repaired under load. Constr Build Mater 2010;24:1051–9.
[16] Malumbela G, Alexander MG, Moyo P. Serviceability of corrosion-affected RC beams after patch repairs and FRPs under load. Mater Struct 2010. doi:10.1617/s11527-010-9630-.
[17] South African National Standards. Structural use of concrete-Part 1. Design (SANS 10100-1:2000). Pretoria: The Bureau; 2000.
[18] El Maaddawy T, Soudki K. Model for prediction of time from corrosion initiation to corrosion cracking. Cem Concr Compos 2007;29(3):168–75.
[19] Malumbela G, Alexander MG, Moyo P. Model for cover cracking of RC beams due to partial surface steel corrosion. Constr Build Mater 2010. doi:10.1016/j.conbuildmat.2010.06.08.
[20] Malumbela G, Alexander MG, Moyo P. Lateral deformation of RC beams under simultaneous load and steel corrosion. Constr Build Mater 2010;24:17–24.
[21] François R, Arliguie G. Influence of service cracking on reinforcement steel corrosion. J Mater Civil Eng 1998;10(1):14–20.
[22] DuraCrete. The European Union—Brite EuRam III, DuraCrete final technical report, Document BE95-1347/R17, 2000.